UKACC International Conference on Control 2012
Cardiff, UK, 3-5 September 2012

Robust hybrid fuzzy logic control of a novel two-wheeled robotic vehicle with a movable payload under various operating conditions

A M Almeshal and M O Tokhi
Department of Automatic Control and Systems Engineering
University of Sheffield
Sheffield, United Kingdom
a.m.almeshal@sheffield.ac.uk

K M Goher
Department of Mechanical and Industrial Engineering
Sultan Qaboos University
Muscat, Oman
kgoher@squ.edu.om

Abstract*—A novel design of two-wheeled double inverted pendulum-like vehicle with a movable payload is presented in this paper. The developed design extends the abilities of the vehicle with five degrees of freedom. The increase of degrees of freedom provides the vehicle with more flexibility in maneuvering in narrow spaces and limited travel distances. The dynamic model of the system is derived using Euler-Lagrange approach and simulated in Matlab Simulink environment. A hybrid fuzzy logic control approach is adopted to control and stabilise the vehicle. Various external disturbances are applied to the system to test the robustness of the control approach. It is demonstrated that the proposed controller successfully stabilises the vehicle in the upright position.

Keywords; modelling ; Lagrangian dynamics ; double inverted pendulum ; hybrid control; fuzzy logic control;

I. INTRODUCTION

An extensive amount of research on inverted pendulum (IP) system is found in the literature due its high nonlinearity and under-actuated nature [1]. It has been used as a platform to test various control algorithms as well as a basis to develop various applications. The applications include, but not limited to, gait of humanoid robots, personal transporters, and self-balancing wheelchairs [2]. The IP system exists in many variations such as mobile inverted pendulum on cart and rotational IP systems. In addition, IP systems have been extended to have multiple links to increase the degrees of freedom (DOF); such as double inverted and triple inverted pendulums [3][4][5]. The increased DOF increase the complexity of the system adding more space for new applications to be developed.

A novel configuration of balancing two-wheeled double inverted pendulum-like vehicle with a movable payload has been presented in [1]. The novelty in the configuration relies in the increased degrees of freedom with the ability to lift a payload to a higher extent. Mathematical model of system dynamics has been derived and presented in [2]. A hybrid fuzzy logic control (FLC) approach is developed to control the vehicle. The vehicle model is used as a basis for an ongoing research of new type of self-balancing wheelchairs with an extended height and ability to maneuver on irregular and uneven surfaces.

II. SYSTEM DESCRIPTION AND MATHEMATICAL MODEL

A schematic diagram of the designed vehicle is shown in Figure 1. The vehicle is designed based on the double inverted pendulum system model with novel modifications [1]. The vehicle consists of two links and a cart driven by two DC motors that in turn drive the entire system. A third DC motor is used to drive the second link. These motors will help stabilizing the system in the upright position by applying an appropriate control signal. The second link consists of two co-axial rods connected by a linear actuator to enable lifting up the payload to a demanded height. Therefore, the system has five degrees of freedom; translational motion with the right and left wheels, first and second links and linear actuator on the second link. The tilt angles of the first and second links are θ_1 and θ_2 respectively. The linear displacement of the payload designated as Q, while the angular displacements of the left and right wheels designated as δ_L and δ_R respectively.

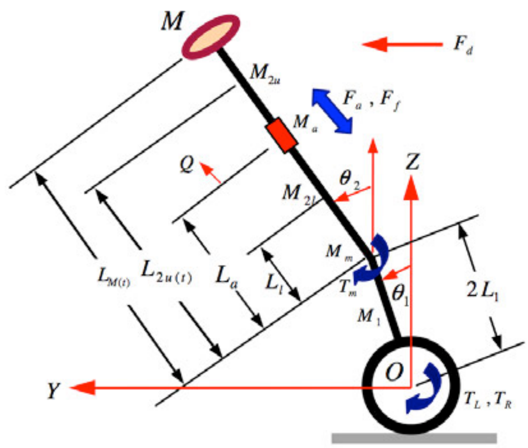

Figure 1. Schematic description of the vehicle

Table 1 describes system model terms and parameters. The system mathematical model consists of five differential equations. The system was modeled using Euler-Lagrange approach because of the system complexity and high coupling nature. System equations of motion were derived in detail in [2] and are presented as in equations (1-5).

Variable	Description	Unit
$L_{M(t)}$	Distance to the COM of the payload	m
$L_{2u(t)}$	Distance to the COM of the upper part link 2	m
L_a	Position of the linear actuator	m
L_l	Half length of link 1	m
Q	Displacement of the linear actuator	m
M_1	Mass of link 1	kg
M_m	Mass of motor driving link 2	kg
M_{2l}	Mass of the lower part of link 2	kg
M_a	Mass of the linear actuator	kg
M_{2u}	Mass of the upper part of link 2	kg
M	Payload mass	kg
T_R, T_L	Right and left wheels driving torques	N.m
T_m	Motor torque	N.m
F_f	Frictional force in the linear actuator	N
F_d	External disturbance force	N
θ_1	Angular position of link 1 to the positive Z axis	rad
θ_2	Angular position of link 2 to the positive Z axis	rad
ϕ	Yaw angle of the vehicle around the Z axis	rad
δ_R , δ_L	Angular position of the right and left wheels	rad
J_l	Mass moment of inertia of link 1	$kg.m^2$
J_{2u}	Mass moment of inertia of the upper rod of link 2	$kg.m^2$
J_a	Mass moment of inertia of the actuator	$kg.m^2$
J_M	Mass moment of inertia of the payload	$kg.m^2$
J_w	Mass moment of inertia of the wheels	$kg.m^2$
J_{IB}	Mass moment of inertia of the intermediate body	$kg.m^2$
J_{2L}	Mass moment of inertia of the lower rod of link 2	$kg.m^2$

Table 1. Nomenclature

$$\begin{aligned}&2C_{21}\ddot{\delta}_L + C_{22}\ddot{\delta}_R + C_9\frac{R_w}{2}L_1\ddot{\theta}_1\cos\theta_1 - C_9\frac{R_w}{2}L_1\dot{\theta}_1^2\sin\theta_1\\&+\frac{R_w}{2}(C_{10}+C_8Q)\ddot{\theta}_2\cos\theta_2 - \frac{R_w}{2}(C_{10}+C_8Q)\dot{\theta}_2^2\sin\theta_2\\&+\frac{R_w}{2}C_8\dot{Q}\dot{\theta}_2\cos\theta_2 = T_L - T_{fL}\end{aligned} \tag{1}$$

$$\begin{aligned}&2C_{21}\ddot{\delta}_R + C_{22}\ddot{\delta}_L + C_9\frac{R_w}{2}L_1\ddot{\theta}_1\cos\theta_1 - C_9\frac{R_w}{2}L_1\dot{\theta}_1^2\sin\theta_1\\&+\frac{R_w}{2}(C_{10}+C_8Q)\ddot{\theta}_2\cos\theta_2 - \frac{R_w}{2}(C_{10}+C_8Q)\dot{\theta}_2^2\sin\theta_2\\&+\frac{R_w}{2}C_8\dot{Q}\dot{\theta}_2\cos\theta_2 = T_R - T_{fR}\end{aligned} \tag{2}$$

$$\begin{aligned}&2C_{18}\ddot{\theta}_1 + C_9\frac{R_w}{2}L_1(\ddot{\delta}_L+\ddot{\delta}_R)\cos\theta_1 - C_9\frac{R_w}{2}L_1(\dot{\delta}_L+\dot{\delta}_R)\dot{\theta}_1\sin\theta_1\\&+2L_1(C_{10}+C_8Q)\ddot{\theta}_2\cos(\theta_1-\theta_2) - 2L_1(C_{10}+C_8Q)\dot{\theta}_1\dot{\theta}_2\sin(\theta_1-\theta_2)\\&+2L_1(C_{10}+C_8Q)\dot{\theta}_2^2\sin(\theta_1-\theta_2) + 2L_1C_8\dot{Q}\dot{\theta}_2\cos(\theta_1-\theta_2)\\&+C_9\frac{R_w}{2}L_1\dot{\theta}_1^2(\dot{\delta}_L+\dot{\delta}_R)\sin\theta_1 + 2L_1(C_{10}+C_8Q)\dot{\theta}_1^2\dot{\theta}_2\sin(\theta_1-\theta_2)\\&-C_3g\dot{\theta}_1\sin\theta_1 = \frac{1}{2}(T_{LT}+T_{RT})\end{aligned} \tag{3}$$

$$\begin{aligned}&C_{20}\ddot{\theta}_2 + (C_{12}\dot{Q} + 2C_8Q)\dot{\theta}_2 + (C_{12}Q + C_8Q^2)\ddot{\theta}_2\\&+\frac{R_w}{2}(C_{10}+C_8Q)(\ddot{\delta}_L+\ddot{\delta}_R)\cos\theta_2\\&-\frac{R_w}{2}(C_{10}+C_8Q)(\dot{\delta}_L+\dot{\delta}_R)\dot{\theta}_2\sin(\theta_2)\\&+C_8\frac{R_w}{2}\dot{Q}(\dot{\delta}_L+\dot{\delta}_R)\cos\theta_2 + 2L_1(C_{10}+C_8Q)\ddot{\theta}_1\cos(\theta_1-\theta_2)\\&-2L_1(C_{10}+C_8Q)\dot{\theta}_1^2\sin(\theta_1-\theta_2) + 2L_1(C_{10}+C_8Q)\dot{\theta}_1\dot{\theta}_2\sin(\theta_1-\theta_2)\\&+2C_8L_1\dot{\theta}_1\dot{\theta}_2\cos(\theta_1-\theta_2) + \frac{R_w}{2}(C_{10}+C_8Q)(\dot{\delta}_L+\dot{\delta}_R)\dot{\theta}_2^2\sin\theta_2\\&-(C_{15}+C_8Q)g\dot{\theta}_2\sin\theta_2\\&-2L_1(C_{10}+C_8Q)\dot{\theta}_1\dot{\theta}_2^2\sin(\theta_1-\theta_2) = T_M - T_{FM} - L_dF_d\end{aligned} \tag{4}$$

$$\begin{aligned}&C_8\ddot{Q} - \frac{1}{2}(C_{12}+2C_8Q)\dot{\theta}_2^2 - C_8\frac{R_w}{2}\dot{\theta}_2(\dot{\delta}_L+\dot{\delta}_R)\cos\theta_2\\&-2L_1C_8\dot{\theta}_1\dot{\theta}_2\cos(\theta_1-\theta_2) + C_8g\cos\theta_2 = F_a - F_{fa}\end{aligned} \tag{5}$$

III. HYBRID FUZZY LOGIC CONTROL STRATEGY

Two types of hybrid FLC are designed and implemented to control the novel non-linear two-wheeled vehicle with five degrees of freedom and movable payload. Referring to Figure 2, the block diagram of the system is presented. Proportional-Derivative-like fuzzy logic controller (PD-like FLC) is used to control the angular displacement of the wheels, the first link tilt angle and the payload linear actuator displacement. A PD plus integral fuzzy logic controllers (PD+I FLC) are used to control the links tilt angles to overcome the steady-state error.

The inputs to the PD-like FLC are the error signal and the change of error. While the inputs for the PD+I FLC are the error signal, change of error and the sum of previous errors. Figure 2 presents the Simulink block diagram of the controlled system.

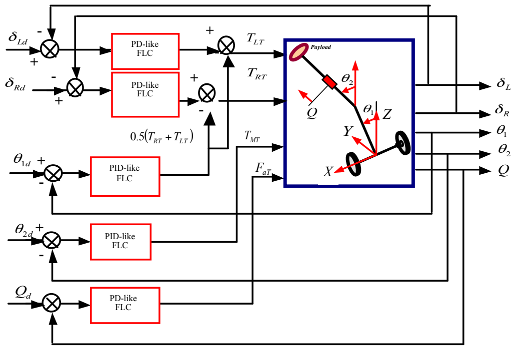

Figure 2. System simulink block diagram

The design of the FLC involves choosing a suitable fuzzy inference engine, defining the fuzzy rules and choosing the membership function type. The FLC developed here is based on Mamdani-type fuzzy inference engine with 25 fuzzy rules presented in Table 2 and Figure 3. The generation of the fuzzy rules-base is based on the required system performance to minimize the system error between the output signal and the desired signal.

Table 2. Fuzzy rule base

e|ê	**NB**	**NS**	**Z**	**PS**	**PB**
NB	NB	NB	NB	NS	Z
NS	NB	NB	NS	Z	PS
Z	NB	NS	Z	PS	PB
PS	NS	Z	PS	PB	PB
PB	Z	PS	PB	PB	PB

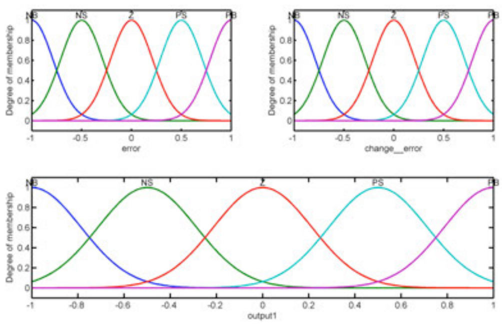

Figure 3. Gaussian fuzzy membership functions

IV. Simulation And Results

In order to test the robustness of the developed control approach, two types of external disturbances were applied to the system. The first simulation scenario incorporates applying disturbances with different amplitudes to the system. The second scenario is to apply disturbances with different durations to the system.

A. Variation of disturbance force amplitudes

Different levels of the applied disturbance force; 0 N, 40 N, 80 N, 160 N, 300 N, were used to examine the robustness of the developed hybrid FLC. The response of the system to the disturbances applied to the centre of the first link and second link are presented in Figures 4 and 5 respectively.

As noted in Figure 4, overshoots resulted in the tilt angle of the first link with a maximum peak amplitude increase of 30% at the maximum disturbance. The average settling time is approximately 5 seconds. The settling time increased by 3% of the initial value with each increase in the disturbance amplitude. Negative peaks at displacements of both wheel motors. Thus explains the opposing movement of the cart to overcome the disturbances and to stabilise the first link at the upright position. The tilt angle of the second link and the displacement of the payload actuator were not affected by this disturbance.

Referring to Figure 5, the effect of applying disturbances to the centre of the second link can be noted. Disturbances resulted in oscillations in the tilt angle of the second link. The tilt angle converges back to the set point within 5 seconds at the maximum applied disturbance force while the rise-time remained unchanged. With every increment of disturbance force amplitude, the peak value increased by an average of 50%. The angular displacements of both wheels, the tilt angle of the first link and the displacement of the payload actuator remained almost unaffected by this disturbance. This is due to the high damping effects caused by the joints of the vehicle and the motor linking the pendulum links.

B. Variation of disturbance force duration

Different durations of the applied disturbance force; 0 sec, 1.25 sec, 2.5 sec, 7.5 sec, 12.5 sec, with a fixed force amplitude of 40 N were used. The response of the system to the disturbances applied to the centre of the first and second links are presented in Figures 6 and 7 respectively.

As noted in Figure 6, oscillations were observed at the tilt angle of the first link with varied amplitudes. The longer the applied disturbance duration the larger the amplitudes of oscillations were noted. The settling-time increased by an average of 6% while the rise-time varied by increasing and decreasing depending on the duration of the applied disturbance. The right and left wheel angular displacements were affected by this disturbance and fluctuations can be noted. The tilt angle of the second link and the payload actuator displacement were not affected by this disturbance.

Figure 7 shows the response of the system for disturbances applied at the centre of the second link. The disturbances resulted in an oscillatory response at the tilt angle of the second link; at disturbance durations up to 7.5 seconds, the controller was able to control the tilt angle of the second pendulum and stabilise the system within an approximate average times of 7 seconds. Settling-time increased by an average of 7% at a time. Finally, The right and left wheel angular displacements, tilt angle of the first link and the payload actuator displacement were not affected by this disturbance.

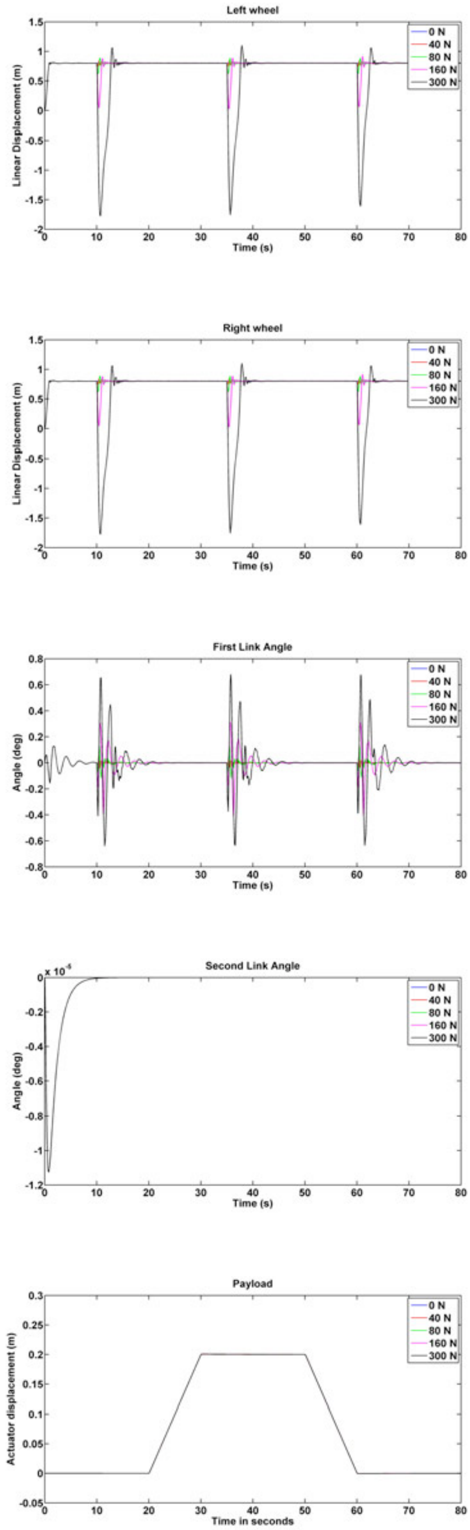

Figure 4. System performance with disturbances
Of different amplitudes applied at the centre of 1st link

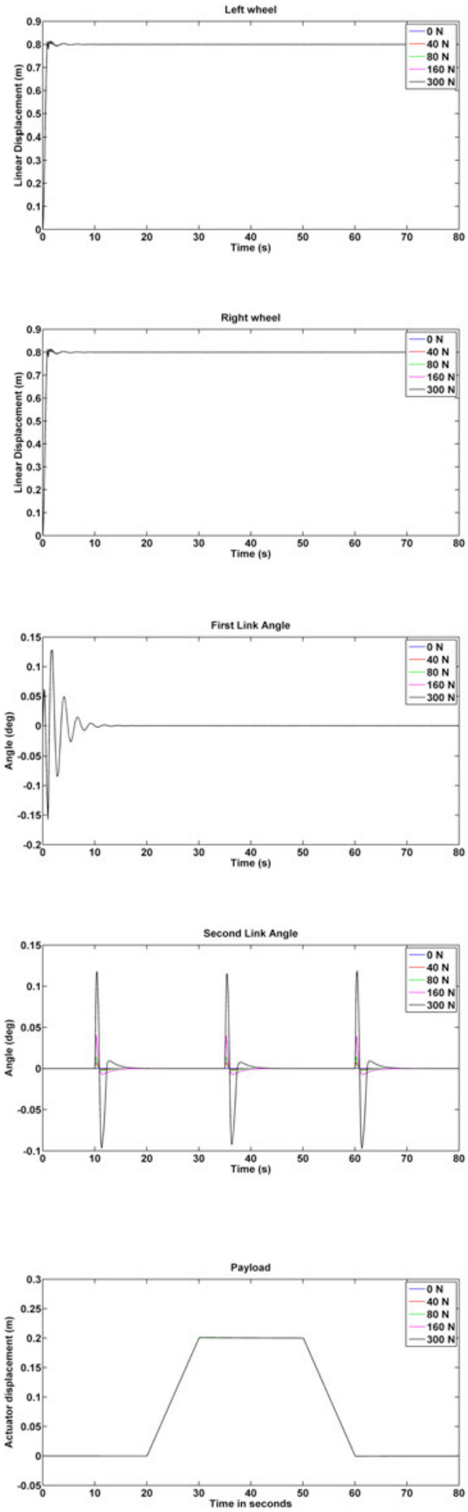

Figure 5. System performance with disturbances
Of different amplitudes applied at the centre of 2nd link

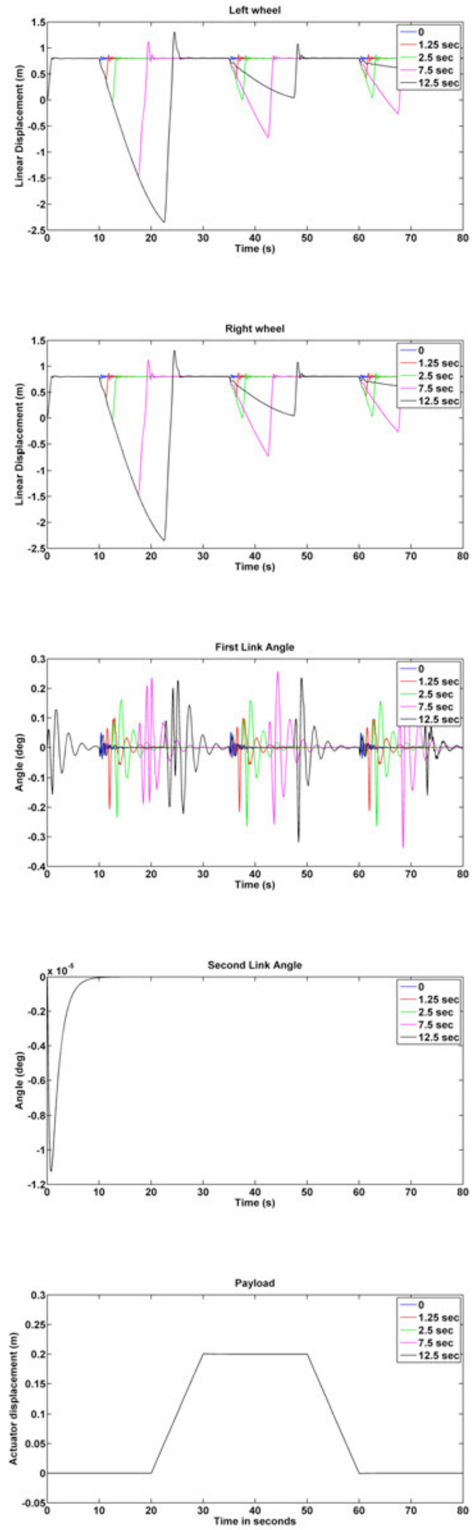

Figure 6. System performance with disturbances
Of different durations applied at the centre of 1st link

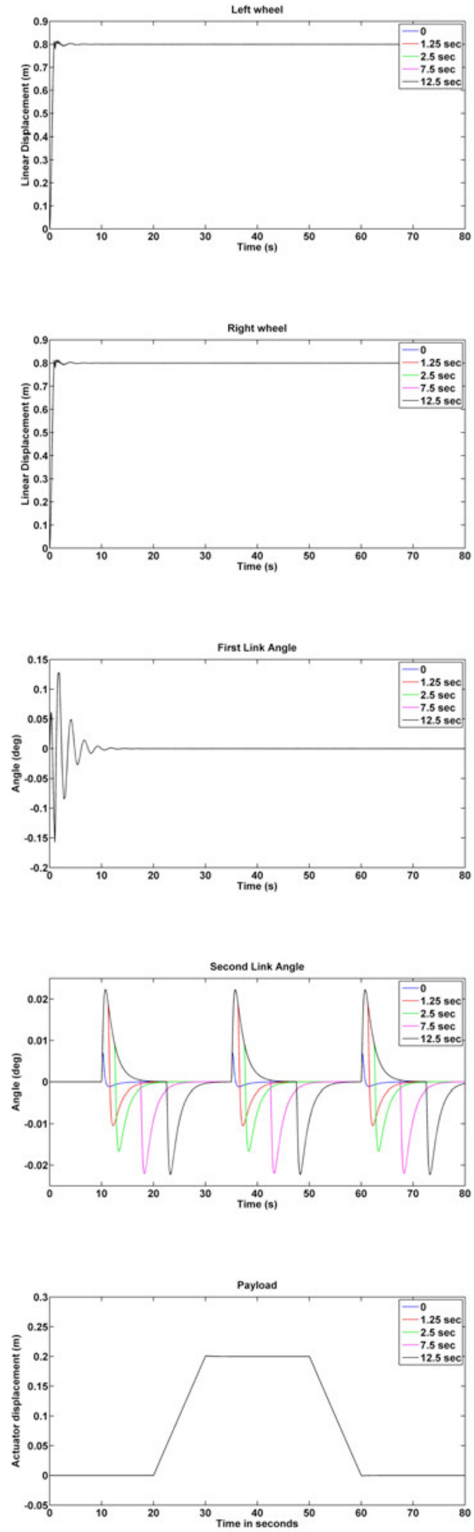

Figure 7. System performance with disturbances
Of different durations applied at the centre of 2nd link

V. CONCLUSION

A hybrid fuzzy logic control approach has been designed and applied on a novel configuration of two-wheeled robotic vehicle. The mathematical model of the vehicle with five degrees of freedom has been derived and equations of motion presented. The model was simulated in Matlab Simulink environment and successfully stabilised. Simulations of the system undergoing different disturbance scenarios have been demonstrated and it has been proved that the controller is able to balance the vehicle in the upright position with various disturbances. The developed hybrid FLC mechanism has been shown to be robust and overcoming external impacts of disturbances.

REFERENCES

[1] K. Goher, S. Ahmad, M. O. Tokhi, A new configuration of two wheeled vehicles: Towards a more workspace and motion flexibility, Proceedings of 4th Annual IEEE conference on Intelligent Systems, San Diego, CA, USA, 5-8 April 2010.

[2] A. M. Al-Meshal, K. M. Goher, M.O. Tokhi, (2011, 8-10 September), Modelling of two-wheeled robotic wheelchair with moving payload. Proceedings of the 14th International Conference on Climbing and Walking Robots and the Support Technologies for Mobile Machines (CLAWAR 2011), Paris, France.

[3] K.G. Eltohamy, and C.Y. Kuo, Real time stabilisation of a triple link inverted pendulum using single control input , IEE Proceedings on Control Theory and Applications , vol.144, no.5, pp.498-504, Sep 1997.

[4] S. Ahmad S., M.O. Tokhi, Modeling and Control of a Wheelchair on Two Wheels, Second Asia International Conference on Modeling & Simulation, 2008. AICMS 08. ,pp.579-584, 13-15 May 2008.

[5] L. Yang, Y. Zhang, Bilinear control for the triple inverted pendulum based on model bias separation, Computer and Automation. 5 (2010) 436-440.